

Transient measurements on miniaturized diaphragm pumps in microfluid systems

R. Zengerle, W. Geiger, M. Richter, J. Ulrich, S. Kluge, A. Richter

Fraunhofer-Institut für Festkörpertechnologie, Hansastrasse 27d, D-80686 Munich, Germany

Abstract

In this paper the dynamics of miniaturized diaphragm pumps will be investigated by transient pressure measurements on the millisecond time scale. The results will be compared with simulations. It will be shown that there is a strong interaction between the dynamics of miniaturized diaphragm pumps and the geometry of the connected fluid channels, caused by the inertia of the fluid.

Keywords: Microfluid systems; Miniaturized diaphragm pump

1. Introduction

During the past few years, many miniaturized fluidic components like micropumps, flow sensors, active and passive valves as well as chemical sensors have been developed [1,2]. Combining these elements, a lot of applications in the field of chemical process control, medical drug delivery systems, environmental control, consumer goods and industrial equipment are becoming possible. As a first application miniaturized diaphragm pumps were integrated with flow sensors [3,4]. This led to an internal feedback system which allows a fluid control in the $\mu\text{l}/\text{min}$ range, with smallest dead volumes and fast response times. Nevertheless little is known about the complex dynamic interaction between these types of micropumps and the fluid in the connected fluid system. Transient pressure measurements on such systems will be presented in this paper in order to investigate the interaction.

2. Dynamics of miniaturized diaphragm pumps

Miniaturized diaphragm pumps consist of an actuated diaphragm, driven by different actuation mechanisms, and two passive check valves [5–8] or diffusor/nozzle elements [9]. At first sight, the pumps resemble very much their macroscopic equivalents. However, there is a large difference in the dynamic behaviour between macroscopic and microscopic pump devices. The pump rate Φ of macroscopic reciprocating pumps is given by

the externally forced volume stroke V_H of a piston (or a diaphragm) and the operation frequency f ($\Phi = fV_H$). But in the case of miniaturized diaphragm pumps, only the forces acting on the driving diaphragm can be controlled by the operator. The volume stroke of the driving diaphragm depends on the hydrostatic pressures on the inlet and outlet side of the pump, the operation frequency and the properties of the passive check valves. Miniaturized diaphragm pumps therefore have to be handled as complex subsystems of fluid networks.

We developed an analytical model for the dynamic behaviour of miniaturized diaphragm pumps [10,11]. A schematic view of the model is depicted in Fig. 1. The coupling between the different pump elements (microvalves and driving diaphragm) and the fluid as well as elastic elements outside the pump are taken into account.

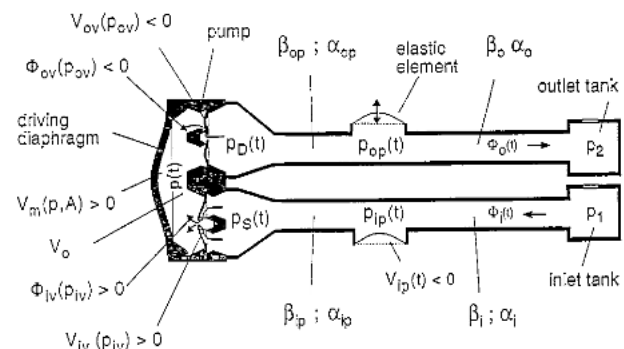


Fig. 1. General simulation model for the dynamic of miniaturized diaphragm pumps, connected with flow channels and elastic elements ($p_{ov} = p - p_D$; $p_{iv} = p_S - p$).

The microvalves of the pump in this model are described by their static flow characteristic $\Phi_{iv/ov}$ and their static volume deformation $V_{iv/ov}$, both are pressure dependent. The driving diaphragm is characterized by the quasi-static function $V_m(p, A)$. It describes the coupling between the volume displacement of the driving diaphragm and the resulting pressure p inside the pump chamber at a given actuation condition $A(t)$. In the case of electrostatic actuation, $A(t)$ equals the electrostatic supply voltage U [11]. The flow channels connected with the pump are described by their flow characteristics and the inertia of the fluid inside the channel. The laminar pressure loss $p_{laminar}$ across a fluid channel, caused by a volume flow Φ , equals:

$$p_{laminar} = \rho \beta \Phi \quad (1)$$

where β is the fluid resistance of the channel and ρ is the density of the fluid. The dynamic pressure loss p_{inert} caused by the inertia of the fluid depends on the transient change in the volume flow Φ and can be calculated as:

$$p_{inert} = \rho \alpha \frac{d\Phi}{dt} \quad (2)$$

where α is the fluid inductance of the flow channel and is given by $\alpha = 4L/(3S)$, where L is the length and S the cross section of the flow channel. Elastic elements outside the pump are characterized by their pressure-dependent volume deformation which can be seen as a fluid capacitance C :

$$C_{ip/op} = \rho \frac{dV_{ip/op}}{dp_{ip/op}} \quad (3)$$

The analytical description of the pump dynamics within this model leads to a system of five coupled nonlinear differential equations which are describing the transient behaviour of the five independent pressure variables p , p_s , p_D , p_{ip} and p_{op} (see Fig. 1). These equations and their solution using a numerical simulation tool called PUSI, are published in Ref. [13].

3. Transient pressure measurements

Transient pressure measurements were carried out in order to confirm the validity of the theoretical model. Firstly measurements in a simplified model system will be discussed in order to demonstrate the important influence of the flow resistance of microvalves and the geometry of fluid channels on the dynamics of miniaturized diaphragm pumps. The model system is depicted in Fig. 2.

An electrostatic or pneumatic actuation unit and a miniaturized pressure sensor were fitted in a Perspex housing. For the pressure measurements, the deflection

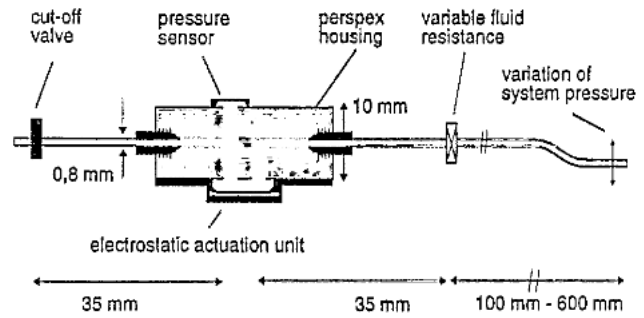


Fig. 2. Experimental setup for transient pressure measurements in a simplified model.

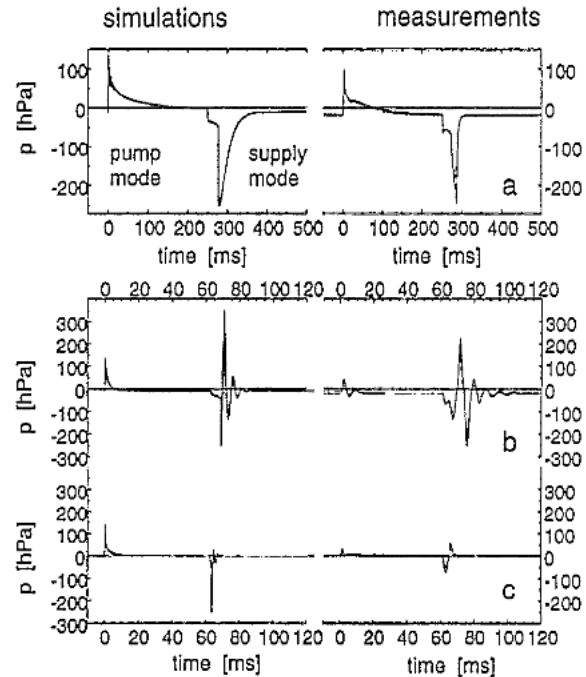


Fig. 3. Transient measurements and simulations using an electrostatically actuated pump diaphragm, driven by a square wave supply voltage of 200 V. (a) $L=600$ mm, radius=0.4 mm, system pressure=-20 hPa, $f=2$ Hz; (b) $L=600$ mm, radius=0.4 mm, system pressure=-20 hPa, $f=8$ Hz; (c) $L=100$ mm, radius=0.4 mm, system pressure=0 hPa; $f=8$ Hz.

of a 800 μm wide and 0.4 μm thick silicon carbide diaphragm was detected by an optical measurement system providing a time resolution of 0.4 ms. In order to test different fluid resistances of microvalves, the microvalves were substituted by variable flow restrictions. The fluid resistance of these elements can be changed quickly.

Transient measurements on an electrostatically actuated model system (driving voltage 200 V) are depicted in Fig. 3. At a high fluid resistance of the variable flow restriction ($\rho\beta=1.25$ hPa min/ μl) and a tube length of 600 mm, there is no influence of the peripheral fluid system (Fig. 3(a)). The signals during the supply mode and pump mode are not symmetrical. This is typical for an electrostatic actuation. A shoulder in the transient signal of the supply mode is also a characteristic feature of an electrostatically actuated diaphragm pump at some special parameter constellations. (For a better

resolution of the characteristic shoulder a reduced system pressure of -20 hPa has been chosen.) In Fig. 3(b) the fluid resistance of the variable flow restriction has been reduced to a value which is equal to the fluid resistance of microvalves in miniaturized diaphragm pumps in forward direction ($\rho\beta = 0.05$ min hPa/ μ l). The transient behaviour changes completely and the pressure signal during the supply mode is dominated by oscillations. These oscillations are typical for the influence of the inertia of the fluid in the tubes connected with the micropump.

The behaviour of the system can be understood by mechanical analogy. The driving diaphragm can be seen as a spring which is coupled with the inert fluid mass in the fluid channels. The flow resistance of a microvalve works as a damping element. If the flow resistance (damping) of the microvalve is low enough, the system can be stimulated to oscillations.

The small deviations between measurements and simulations in Fig. 3(b) are due to the inertia of the fluid inside the pump chamber. This effect was not simulated in the theoretical model. It is only important because the pump chamber volume is quite large in this special experimental housing. The reduction of the tubing length from 600 to 100 mm is leading to a drastic change in the transient pressure signal (Fig. 3(c)). The oscillations in the pressure signal disappear and all processes become much faster. But unfortunately, the time resolution of our measurement system was not good enough for the detailed resolution of the short pressure peaks.

The transient signals in the case of a pneumatic drive are depicted in Fig. 4. Thereby, the driving diaphragm has been actuated by a pneumatic pressure with an amplitude of -200 hPa, generated by an external pneumatic system. We used a square wave shape for the transient actuation pressure with a slope (10 to 90% signal) for switching on/off the pneumatic pressure during the supply/pump mode of 3.5 ms/8.0 ms. The fluid capacitance of the driving diaphragm has been $\rho^{-1}C_m = 0.5$ nl/hPa. Using a fluid resistance of the flow restriction which is quite large ($\rho\beta = 0.625$ min hPa/ μ l), the connected fluid system has no influence on the dynamics (Fig. 4(a)). In contrast, at a low fluid resistance ($\rho\beta = 0.03$ min hPa/ μ l and $\rho\beta = 0.005$ min hPa/ μ l), oscillations of the pressure signal can be seen (Fig. 4(b) and (c)). They are caused by the coupling between the fluid inductance of the flow channel and the fluid capacitance of the driving diaphragm. This demonstrates that the inertia of fluid has to be taken into account, whenever the fluid resistance of the microvalves is low enough and the time constants for turning on/off the actuation forces are of the same order as the time constants, caused by the fluid inductance of the fluid channels. The inertia effects are more important when the time constants for changing

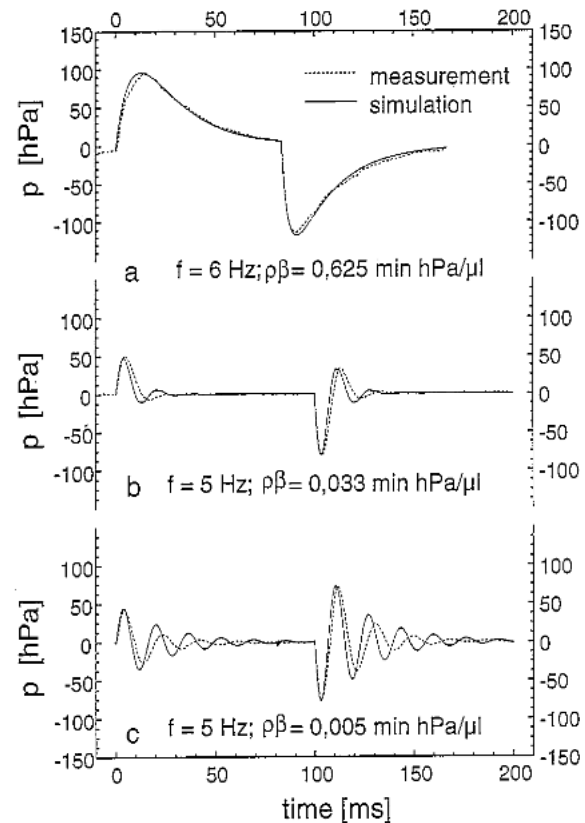


Fig. 4. Transient measurements and simulations using a pneumatically driven actuation unit, tube radius = 0.4 mm; tube length = 600 mm.

the actuation pressure by the external pneumatic system are small. This can be seen by comparing the transient signals of supply mode (3.5 ms) and pump mode (8 ms) (Fig. 4(b)).

It is possible to give a criterion that describes the appearance of oscillations in the pressure signal in this simple measurement setup, if all fluid resistances and fluid capacitances are kept constant. It depends on the fluid resistance β_c and the fluid inductance α_c of the flow channel, the fluid resistance β of the flow restriction as well as the fluid capacitance C_m of the driving diaphragm:

$$(\beta_v + \beta_c)^2 < \frac{4\alpha_c}{C_m} \quad (4)$$

As have been shown, the transient measurements in the simplified model system are in good agreement with the simulations. In a next step, it is very interesting to look at the transient pressure signals in micropumps with two passive check valves. The corresponding experimental setup is given in Fig. 5. Two passive check valves are embedded in a Perspex housing. The design of the valves and the driving unit equals the standard design of the electrostatically actuated micropump [13]. Three pressure sensors are used in order to measure the transient pressures p , p_{ip} and p_{op} .

The transient pressure signals are depicted in Fig. 6. There are two remarkable features: firstly the oscillations in the pump chamber pressure have the same

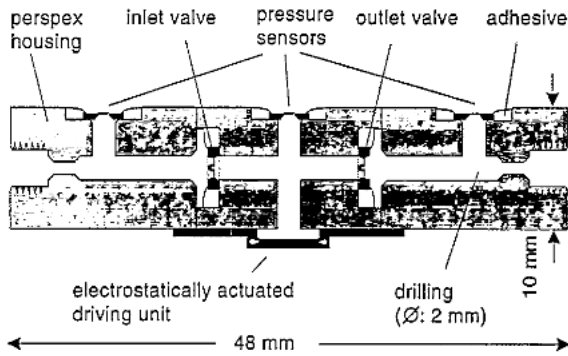


Fig. 5. Experimental setup for transient pressure measurements in miniaturized diaphragm pumps (including dynamic valves).

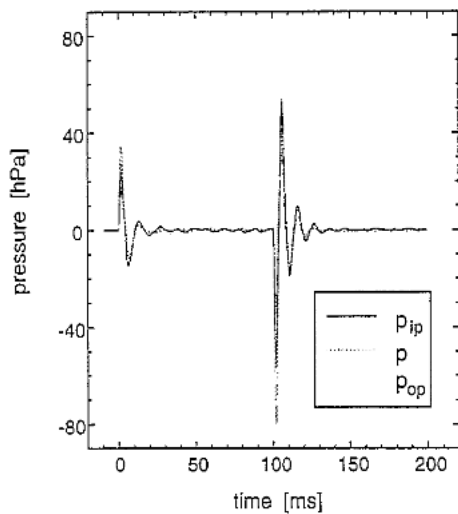


Fig. 6. Transient measurements inside and outside the pump chamber of an electrostatically actuated diaphragm pump.

basis signal shape as those given in Fig. 3(b). But the amplitude of the signal is lower. Secondly, it is very interesting that the pressure signals in the pump chamber as well as outside the pump are almost similar. A coupling between the driving diaphragm and the inlet tube would be expected only during the supply mode of the pump, and a coupling between the driving diaphragm and the outlet tube would only be expected during the pump mode. Comparison with the simulations shows that two effects can be responsible for the equality of the three pressure signals: the volume displacement of microvalves in reverse direction or valve leakage. By each of these effects, the dynamic interaction between the fluid capacitance of the driving diaphragm and the fluid inductance of the inlet channel during the supply mode of the pump can be transferred to the outlet channel and vice versa. All pressure signals equals therefore very much, but nevertheless a pump rate can be measured. In the sample, depicted in Fig. 6, the leakage rates of the microvalves have been measured and were negligible.

The simulations (not depicted here) show a good qualitative agreement, but are leading to larger amplitudes than those that have been measured. Further

experiments with an improved experimental setup are in progress in order to confirm the results depicted in Fig. 6. In these experiments we will also use other types of microvalves (flap valves).

4. Conclusions

The experiments evidenced that there is an interaction between the dynamics of miniaturized diaphragm pumps and the fluid inductance of the flow channels connected with the pump. If the fluid resistance of the microvalves is low enough, this interaction leads to oscillations of the pressure signal inside as well as outside the pump chamber. The frequency and the amplitudes of these oscillations depend mainly on the fluid inductance of the flow channels, the fluid capacitance of the driving diaphragm and the fluid resistances of the microvalves. Therefore, if a certain micropump is placed in different fluid systems, this results, in general, in a different pump performance, specially at operation frequencies above 50 Hz.

The interaction can be decoupled if elastic elements outside the pump chamber are used with a fluid capacitance which is much larger than the fluid capacitance of the driving diaphragm (Fig. 1). Thereby, the oscillations in the pressure signal are smoothed and the oscillations in fluid flow are converted to a continuous flow behind these elements.

The dynamics of the pump model depicted in Fig. 1 can be calculated by the use of the simulation tool PUSI [11]. For driving frequencies between 100 and 200 Hz, we found a very good qualitative agreement and a good quantitative agreement between measurements and simulations. The agreement covers a large range of parameters for the fluid resistances: the fluid capacitances and the fluid inductances of the system components of electrostatically and pneumatically actuated miniaturized diaphragm pumps. If driving frequencies of some hundreds Hz were used, the dynamics of a miniaturized diaphragm pump can be predicted only qualitatively. For driving frequencies higher than 1 kHz a more detailed model has to be used because the inertia of the elastic components (for example resonances of the elastic valve parts) has to be taken into account [14].

Using the simulation tool PUSI, the performance of an electrostatic actuated diaphragm pump with the outer dimensions of 7 mm × 7 mm × 2 mm could be optimized [12]. Until now, a maximum hydrostatic pressure of 350 hPa (3.5 m H₂O) and maximum pump rates of 800 μl/min have been achieved with a supply voltage of 200 V and with actuation frequencies in the range between 1 and 900 Hz. The total power consumption of the pump is frequency dependent and less than 1–10 mW.

Acknowledgements

The work was partly funded by Brite/Euram contract BRE2-CT92-0145 'Design Methodology for Microengineered Fluid Devices'. The authors would also like to thank S. Thoma for the fabrication of the device.

References

- [1] P. Gravesen, J. Branebjerg and O.S. Jensen, Microfluidics, *J. Micromech. Microeng.*, 3 (1993) 168-182.
- [2] C. Cammann, U. Lemka, A. Rohen, J. Sander, H. Wilken and B. Winter, Chemo- und Biosensoren-Grundlagen und Anwendungen, *Angew. Chem.*, 5 (1991) 519-541.
- [3] V. Gass, B.H. van de Schoot, S. Jeanneret and N.F. de Rooij, Integrated flow-regulated silicon micropump, *Proc. Transducer '93, Yokohama, Japan, 7-10 June 1993*, pp. 1048-1051.
- [4] T.S.J. Lammerink, M. Elwenspoek and J.H.J. Fluitman, Integrated micro-liquid dosing system, *Proc. MEMS '93 Workshop, Ford Lauderdale, FA, USA, 7-10 Feb. 1993*, pp. 254-259.
- [5] H.T.G. van Lintel, F.C.M. van de Pol and S. Bouwstra, A piezoelectric micropump based on micromachining of silicon, *Sensors and Actuators*, 15 (1988) 153-167.
- [6] F.C.M. van de Pol, H.T.G. van Lintel, M. Elwenspoek and J.H.J. Fluitman, A thermo-pneumatic micropump based on micro-engineering techniques, *Sensors and Actuators*, A21-A23 (1990) 198-202.
- [7] R. Zengerle, A. Richter and H. Sandmaier, A micro membrane pump with electrostatic actuation, *Proc. MEMS '92, Travemünde, Germany, 4-7 Feb. 1992*, pp. 19-24.
- [8] P. Dario, M.C. Carozza, N. Croce and B. Magnani, A piezoelectric micropump realized by stereolithography, *Proc. Actuator '94, 15-17 June 1994*, pp. 42-45.
- [9] E. Stemme and G. Stemme, A valveless diffuser/nozzle-based fluid pump, *Sensors and Actuators A*, 39 (1993) 159-167.
- [10] R. Zengerle, M. Richter, F. Brosinger, A. Richer and H. Sandmaier, Performance simulation of microminiaturized membrane pumps, *Proc. Transducer '93, Yokohama, Japan, 7-10 June 1993*, pp. 106-109.
- [11] R. Zengerle and M. Richter, Simulation of microfluid systems, *J. Micromech. Microeng.*, 4 (1994) 192-204.
- [12] R. Zengerle, W. Geiger, M. Richter, J. Ulrich, S. Kluge and A. Richter, Application of micro diaphragm pumps in microfluid systems, *Proc. Actuator '94, Bremen, Germany, 15-17 June 1994*, pp. 25-29.
- [13] R. Zengerle, Mikro-Membranpumpen als Komponenten für Mikro-Fluidsysteme, *Ph.D. Thesis*, Universität der Bundeswehr, München, Germany, 1994.
- [14] R. Zengerle, S. Kluge, M. Richter and A. Richter, A bidirectional silicon micropump, *Proc. MEMS '95, Amsterdam, Netherlands, 29 Jan.-2 Feb., 1995*, pp. 19-24.